

STRUCTURAL, OPTICAL AND PHOTO-CATALYTIC ACTIVITY OF Nb-DOPED NiO THIN FILMS

A. A. FARGHALI^{a*}, W. M. A. EL ROUBY^a, M. SH. ABDEL-WAHAB^{a,b}

^a*Materials Science and Nanotechnology Department, Faculty of Postgraduate Studies for Advanced Sciences(PSAS), Beni-Suef University, Beni-Suef, Egypt*

^b*Center of Nanotechnology, King Abdulaziz University, Jeddah-21589, Saudi Arabia*

In this study, structural and optical properties of 0 and 4 wt% Nb-doped NiO thin films deposited by DC/RF magnetron sputtering technique at different substrate temperatures were studied. XRD patterns display peaks corresponding to pure trigonal NiO, No other peaks were noticed that is reflects well dispersion of Nb nanoparticles on the lattice of NiO thin films. Both intensity of photoluminescence (PL) and optical band gap have been greatly affected by Nb-doping and substrate temperatures. The photo-catalytic degradation of MG dye using the doped thin films under visible light showed that Nb-doping and increasing the substrate temperatures plays a significant role to increase the photo-catalytic efficiency from 67, 80 to 100 % within 3 hrs for the films prepared at 25 (Room temperature), 100 and 200 °C respectively. For getting the kinetics parameters, pseudo first order kinetics was applied.

(Received May 11, 2016; Accepted August 3, 2016)

Keywords: NiO; Nb; Photo-catalytic activity

1. Introduction

Photo-catalysis considered as a promising technique for the purification and decontamination of wastewater from organic dyes using semiconductor materials as a photo-catalyst because it is nontoxic, thermally and chemically stable in the presence of light [1-2]. Among these semiconductor materials ZnO and TiO₂ in both powder and thin films have been widely studied for their photo-catalytic activity under UV light that is considered as a harmful light [3-6]. NiO has been considered as a p-type semiconductor with a wide band gap of ~ (3.2 to 3.8eV) [7]. But till this moment there are limited studies on the photo-catalytic degradation of the organic dyes using nanocrystalline NiO thin films [8-9]. Due to their promising electrical, optical and chemical stability, Nanocrystalline NiO thin films have been used for many applications like photocathodes for p-type dye sensitized solar cells [10], memory devices [11], buffer layer in organic solar cells [12], light emitting diode [13], electrochromic devices [14], hydrogen sensing[15-16], smart windows [17], photoelectrochemical water splitting [18], organic photovoltaics [19], antiferromagnetism [20], optoelectronic devices [21].Nanocrystalline NiO thin films have been prepared by different physical and chemical routes such as spray pyrolysis [22], Photo-assisted Metal Organic Chemical Vapour Deposition (PA-MOCVD)[23], sol-gel[24], successive ionic layer adsorption and reaction (SILAR)[25], pulsed laser deposition[26], electron beam evaporation [27], RF magnetron sputtering [28], DC reactive magnetron sputtering [29]. Different research articles have been studied the doping of NiO thin films with copper, palladium, indium, tin, lithium and magnesium to enhance both chemical and physical properties of the films [30-35].

In this study, we fabricated pure and Nb-doped NiO thin films on glass substrate at different temperatures by DC/RF magnetron sputtering technique. The deposited films were characterized using different characterization techniques to evaluate the effect of Nb-doping and

*Corresponding author: d_farghali@yahoo.com

substrate temperatures on the structural and optical properties of NiO thin films. The prepared films were tested as a photo-catalyst for the degradation of MG dye as a pollutant model in waste water.

2. Experimental

2.1 Sample preparation

Pure and Nb-doped NiO thin films were prepared by simultaneous DC/RF magnetron sputtering of Ni and Nb in the presence of oxygen gas (O₂) on a glass substrate (DC/RF Magnetron Sputter System, Syskey Technologies, Taiwan). The used glass slides were cleaned using acetone then dried with nitrogen gas before using. We have used high purity (99.999%) Ni (3 × 0.6 inch) and (99.999%) Nb (3 × 0.6 inch) metal targets for the prepared thin films. Table. 1 shows the deposition parameters values used for the deposition of thin films sample.

2.2 Characterization techniques

The structural, surface morphology and optical properties of the deposited pure and Nb-doped NiO thin films were characterized using X- ray diffractometer (Ultima-IV; Rigaku, Japan) with Cu K α radiation of $\lambda = 1.5418 \text{ \AA}$ wavelength working on 40 kV of accelerating voltage and 30mA of current, field emission scanning electron microscope (FESEM) (JSM – 7600F; JEOL – Japan, UV-Visible spectrophotometer (Perkin Elmer, Lambda 750) and the photoluminescence emission spectra were taken by using Fluorescence Spectrophotometer (RF – 5301 PC, Shimadzu, Japan) at room temperature.

Table 1: Deposition parameters of pure and Nb-doped NiO thin films deposited at different substrate temperatures.

No	Deposition parameters	Value
1	Base pressure	9×10^{-6} Torr
2	Operating pressure	5×10^{-3} Torr
3	Deposition time	1200 sec
4	Substrate temperature for the pure NiO thin film.	25 (RT) °C
5	Substrate temperature for the Nb-doped NiO thin films.	25 (RT), 100 and 200 °C
6	DC power for Ni target	200 W
7	RF power for Nb target	30 W
8	Oxygen flow rate	40 SCCM
9	Argon flow rate	20 SCCM
10	Target – substrate distance	14 cm

2.3 Photo-catalytic experiments

The prepared thin films were used as a photo-catalyst for the degradation of methyl green (MG) dye as a pollutant example in waste water. MG solution with 10 ppm concentration was prepared by dissolving a pre calculated amount of the dye in distilled water. Glass reactor containing 100 ml of MG aqueous solution was used to follow the photo-catalytic experiments under continuous stirring to get aerobic conditions essential for photo-catalytic experiments. The reactor was irradiated with 500 W halogen tungsten lamp as a source of visible light (> 400 nm) for 3 hrs. The lamp was placed vertically on the top of reaction reactor at a distance of 30 cm. After 15 min interval, 3 ml of MG solution was withdrawn to check the changes in its concentration by using UV-Visible spectrophotometer (Perkin Elmer, Lambda 750) through following the variation in its characteristic absorption wavelength at around 630 nm. The following equation was used to calculate the degradation efficiency after analysis:

$$Degradation\% = \frac{C_o - C_t}{C_o} \times 100$$

(1)

Where, C_o is the initial concentration of MG (mg/l) and C_t is the concentration of MG at time t during the catalytic reaction (mg/l).

3. Results and discussion

3.1 Structural analysis

The XRD results for the pure and Nb-doped NiO thin films prepared at different substrate temperatures are provided in Fig.1. The deposited films display peaks corresponding to pure trigonal NiO. For the prepared samples, (021), (202), (220), and (223) diffraction peaks (ICDD card no. 01-089-3080) were observed with C2/c space group that is confirm the growth of NiO crystallites along different directions. It is obvious from the XRD results that the doping of Nb nanoparticles to NiO thin films at room temperature results in suppression the intensity for the whole peaks of the NiO then the intensity of the peaks increased by raising the substrate temperature from 100 to 200°C with small shift for the diffraction peak (202) from 42.38, 42.81, 42.67 to 42.46 degree for the pure and Nb-doped NiO thin films deposited at 25, 100 and 200°C substrate temperatures respectively. No other peaks were noticed for Nb that is indicating the smaller percentage of Nb and well dispersion on the surface of NiO thin films [2]. The average crystal size for the deposited films was calculated using the following Scherrer's equation [36-38]:

$$D = 0.94\lambda / \beta \cos \theta \quad (2)$$

Where, D : crystal size, λ : X- ray wave length, β : the broadening of the diffraction peak and θ is the diffraction angle. The structural properties for the pure and Nb-doped NiO thin films at different substrate temperatures were studied using dislocation density δ that is defined as the length of the dislocation line per unit volume and the strain ε that is appeared in the deposited thin films due lattice misfit were calculated according to the following equations [36-38]:

$$\delta = n / D^2 \quad (3)$$

$$\varepsilon = \beta \cos \theta / 4 \quad (4)$$

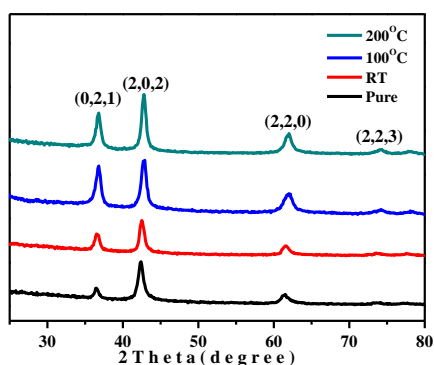


Fig. 1: XRD spectra of pure and Nb-doped NiO thin films deposited at different substrate temperatures.

Table .2 shows the calculated structural parameters such as: average crystallite size, strain and dislocation density. It is obvious that crystallite size for the NiO thin films decreased from

9.91 to 8.81 then increasing from 9.61 to 10.24 for the pure and Nb-doped NiO deposited at 25, 100 and 200°C substrate temperature respectively. Both dislocation density and strain decreases from 1.5, 1.49, 21.22 to 1.06×10^{16} lines/m² and 4.16, 4.13, 3.75 and 3.51×10^{-3} for the pure and Nb-doped NiO deposited at 25, 100 and 200°C substrate temperature respectively that is in good agreement with the reported data for NiO thin films [36-38]. The lower values for dislocation density δ reflect the high quality of the crystallized films.

Table 2: Structural parameters of pure and Nb-doped NiO thin films deposited at different substrate temperatures.

Sample	Crystallite Size (D) (nm)	Dislocation density (δ) (10^{16} lines/m ²)	Strain(ϵ) (10^{-3})
Pure NiO	9.91	1.50	4.16
Nb-doped NiO at RT	8.81	1.49	4.13
Nb-doped NiO at 100 °C	9.61	1.22	3.75
Nb-doped NiO at 200 °C	10.24	1.06	3.51

3.2 Morphology and compositional analysis

The surface morphology and elemental analysis of the pure and Nb-doped NiO thin films at different substrate temperatures were studied by FESEM as shown in Fig.2 (a-d). It can be observed that the morphology and particle size were also greatly influenced by both Nb-doping and changing the substrate temperature. The particle size were increased from 8-10 nm for the pure NiO to 20-25 nm for the Nb-doped NiO thin films at different substrate temperatures which is bigger compared to XRD results. This is can explained on the basis of aggregation of small crystallites with improved crystallinity by increasing the substrate temperature. The EDS spectra for all the deposited pure and Nb-doped NiO thin films clearly show the presence of peaks corresponding to Ni, O, Nb and C elements with 74.9, 15, 4 and 6 wt% respectively.

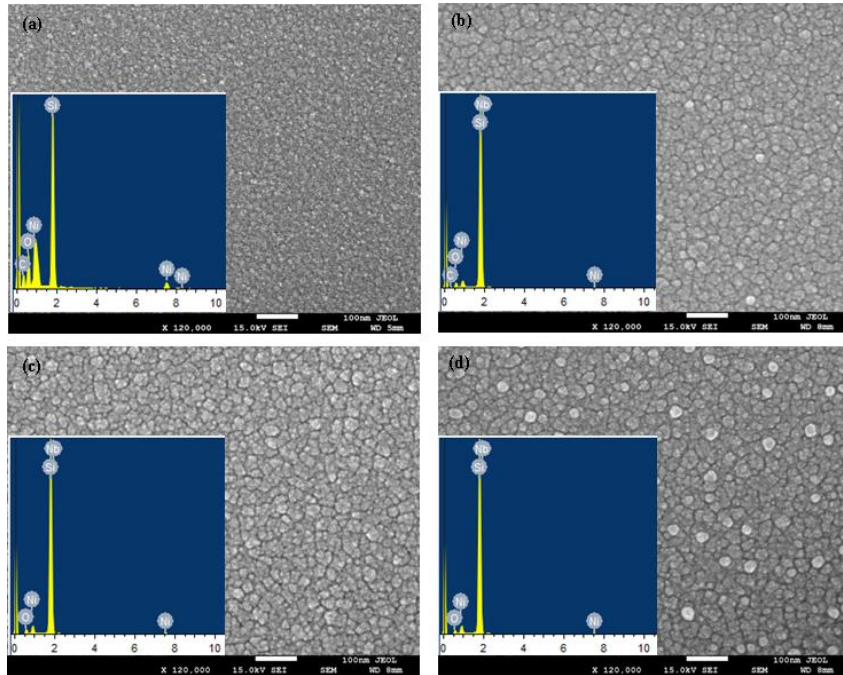


Fig. 2: (a-d): FESEM surface images and EDS spectrum of pure and Nb-doped NiO thin films deposited at different substrate temperatures a) pure NiO, b) RT, c) 100 °C and d) 200 °C.

Fig.3 (a-d) shows the changes of the cross sectional view of the deposited pure and Nb-doped NiO thin films showing a gradual decrease from 80,70,50 to 30 nm by Nb-doping and increasing the substrate temperatures from RT,100 to 200°C which was confirmed for all the deposited films by using surface profiler, DektakXT, Bruker, Germany that is can explained on the basis of reducing the spaces between the particles by Nb-doping and increasing the substrate temperatures which compacting the deposited samples.

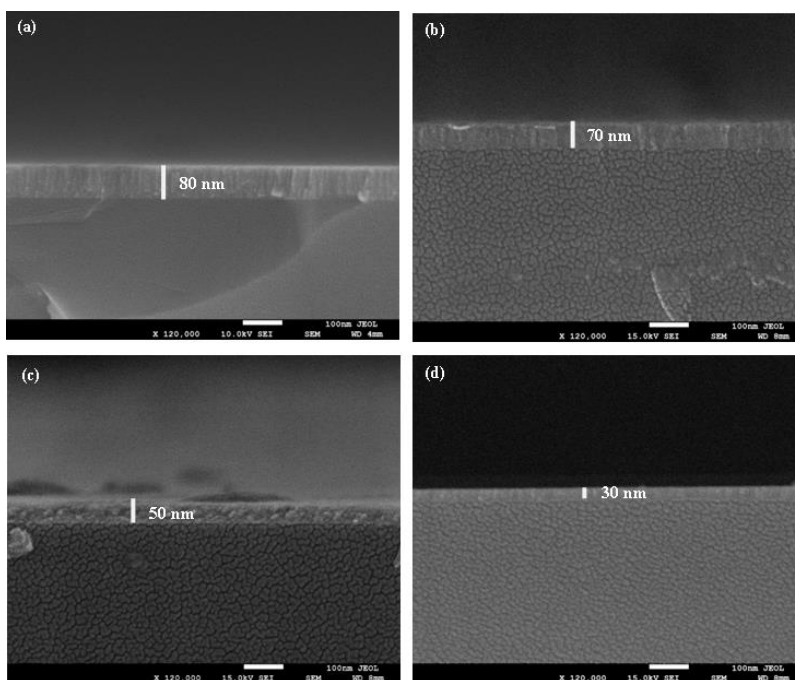


Fig. 3: (a-d): Cross sectional view of pure and Nb-doped NiO thin films deposited at different substrate temperatures a) pure NiO, b) RT, c) 100°C and d) 200 °C.

3.3 Optical properties

UV-visible spectrophotometer was used to record optical absorbance and transmittance in the range of 300 nm to 2400 nm at room temperature to evaluate the influence of Nb-doping and changes in substrate temperature on the optical properties of nanocrystalline NiO thin films.

The optical band gap of pure and Nb-doped NiO thin films at different substrate temperatures was calculated by Tauc's equation [39]:

$$(\alpha h\nu) = A(h\nu - E_g)^n \quad (5)$$

Where, $h\nu$ is the energy of incident photon, α is the absorption coefficient, A is a constant and n may be equals to 1/2 for direct and 2 for indirect band gap and this depends on the quantum selection rules for different materials. In our case, we have used $n = 2$ because it gives an excellent linear fit curve in the band-edge region. The absorption coefficient (α) for pure and Nb-doped NiO thin films can be calculated using the following equation [39]:

$$\alpha = \ln\left(\frac{1}{T}\right)/d \quad (6)$$

Where, d is the thickness of the deposited film and T is the transmittance.

The relation between the $(\alpha h\nu)^2$ vs $h\nu$ for the prepared pure and Nb- doped NiO thin films on glass substrates is clear in Fig.4. The optical band gap for the prepared films decreased from

3.6, 3.48 to 3.42 and 2.99 eV by Nb-doping and increasing the substrate temperature from 100 to 200 °C respectively.

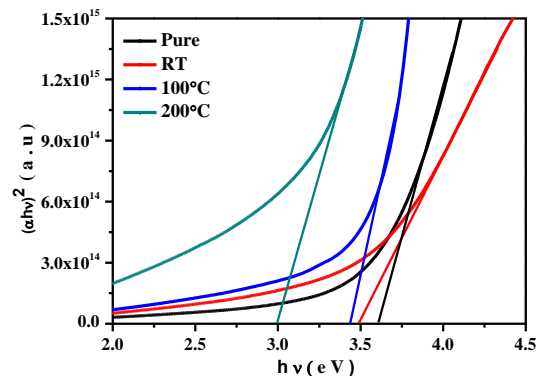


Fig. 4: Variation of optical band gap for pure and Nb-doped NiO thin films.

The PL emission spectra at room temperature of pure and Nb-doped NiO thin films deposited at different substrate temperatures was shown in Fig.5. The results showing sharp peak at 390 nm (3.18 eV, Violet emission) due to the recombination between electrons in conduction band and holes in valence band and a shoulder peak at 470 nm (2.63 eV, Visible emission) due to defects related to oxygen vacancies and Ni interstitials when it is excited with an ultraviolet wavelength $\lambda_{\text{ext}} = 350$ nm that is in good agreements with the results [40]. The PL intensity decreases with Nb-doping and increasing the substrate temperatures. Both optical band gap and PL results will greatly affect the photo-catalytic properties of pure and Nb-doped NiO thin films deposited at different substrate temperatures as we will discuss later.

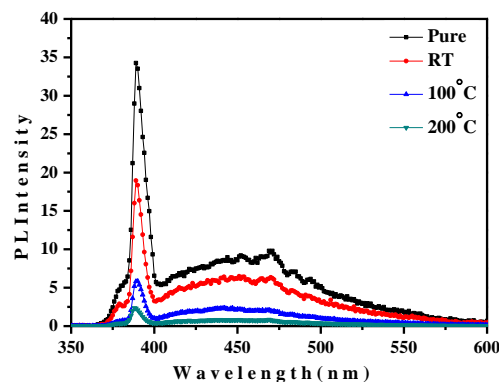


Fig. 5: Photoluminescence spectra for pure and Nb-doped NiO thin films.

3.4 Photo-catalytic experiments

3.4.1 Effect of Nb-doping and substrate temperature on the photo-catalytic efficiency

Fig.6 (a) shows the photo-catalytic degradation of MG dye using pure and Nb-doped NiO thin films at different substrate temperatures. The photo-catalytic experiments were carried out at 10ppm of MG concentration, pH = 6.7 and irradiation time = 3 hrs. It is obvious from the results that the rate of MG dye degradation increased from 25 for the pure NiO sample to 67, 80 and almost 100% by Nb-doping and increasing the substrate temperature from RT, 100 and 200°C. The enhancement of the photo-catalytic activity can be attributed to increasing the e^-/h^+ pair generation and recombination rate that is confirmed from XRD, band gap and PL results that is shows improvement in the NiO thin films crystallinity and decreasing the optical band gap with Nb-doping and increasing the substrate temperature from RT, 100 and 200°C.

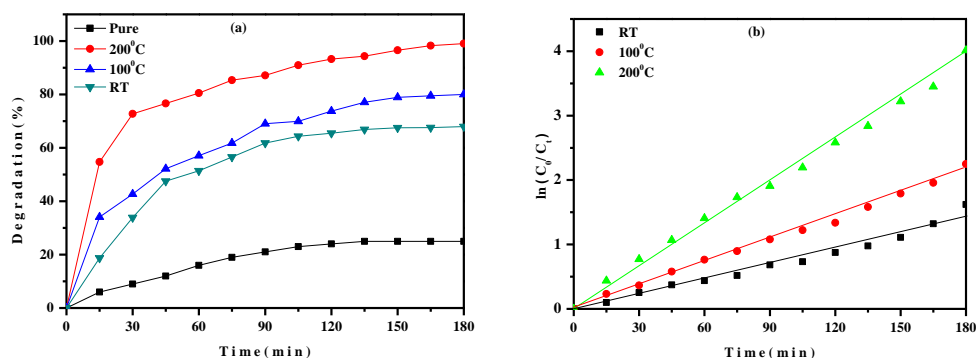


Fig. 6: (a) Effect of Nb- doping / Substrate temperature on the photo-catalytic efficiency, (b) Pseudo – first order decolorization rate constant of MG dye (MG concentration = 10 ppm, visible lamp = 500 W, irradiation time = 3 hrs and pH = 6.7).

To follow the decomposition kinetic of MG dye, Langmuir Hinshelwood kinetics model was applied [2]:-

$$\ln\left(\frac{C_o}{C_t}\right) = k_{app}t \quad (7)$$

Where C_t is the concentration of dye at time t (mg/l), C_o is the initial concentration of the dye (mg/l), and k_{app} is the apparent rate constant (min^{-1}) that is obtained from the slope of the plot between $\ln(C_o/C_t)$ and irradiation time t (min) for the Nb-doped NiO thin films at different substrate temperatures as shown in Fig.6 (b). The calculated degradation rates of MG dye reflects the enhancement from 0.00812, 0.01183 and 0.0209 min^{-1} for the Nb-doped NiO thin films at RT, 100 and 200°C substrate temperature respectively. The results showed that photo degradation of MG dye obeyed the pseudo first order kinetics.

3.4.2 Reusability and stability of deposited Nb-doped NiO thin films

The deposited Nb-doped NiO thin films at different substrate temperatures were used for five times after washing with deionised water and air drying to evaluate its reusability and stability as shown in Fig.7. The results revealed that the change in degradation efficiency ranging from 15-17% after the 5th cycle that is considered as a big advantage for using these films compared to the use of the powder catalysts that are hard to separate, reuse and producing environmental risks.

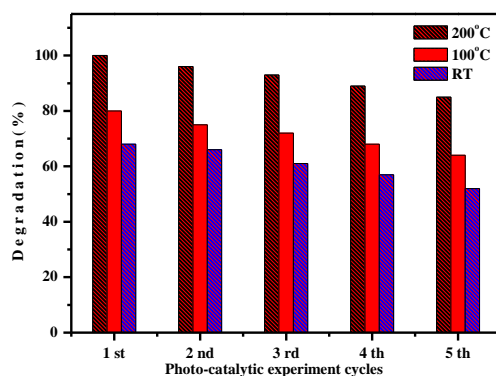


Fig. 7: Reusability of Nb-doped NiO thin film at different substrate temperatures. (MG concentration = 10 ppm, visible lamp = 500 W, irradiation time = 3 hrs and pH = 6.7)

4. Conclusion

Pure and 4 wt% Nb-doped NiO thin films at different substrate temperatures have been prepared by simultaneous deposition of Nb and Ni in the presence of oxygen gas (O₂) on glass substrate by DC/RF magnetron sputtering technique. The prepared thin films were characterized by XRD, FESEM, UV-Visible and PL showing a significant change in the structural, morphological and optical properties by Nb-doping and increasing the substrate temperatures. The photo-catalytic degradation of MG dye has been governed by pseudo first order kinetics with enhancing the efficiency of degradation from 67, 80 to 100% by elevating the substrate temperature from RT, 100 to 200°C.

References

- [1] R. Li, Y. Jia, N. Bu, J. Wu, Q. Zhen, J. Alloys Compd., **643**, 88 (2015).
- [2] F. Bensouici, T. Souier, A. Dakhel, A. Iratni, R. Tala-Ighil, M. Bououdina, Superlattices Microstruct., **85**, 255 (2015).
- [3] N. Talebian, M.R. Nilforoushan, N. Maleki, Thin Solid Films, **527**, 50 (2013).
- [4] N.V. Kaneva, D.T. Dimitrov, C.D. Dushkin, Appl. Surf. Sci., **257**, 8113 (2011).
- [5] W. Vallejo, C. Diaz-Uribe, A. Cantillo, J. Photochem. Photobiol., **A 299**, 80 (2015).
- [6] M. Mohammadzadeh, M. Bagheri, S. Aghabagheri, Y. Abdi, , Appl. Surf. Sci., **350**, 43 (2015).
- [7] R. Sharma, A. Acharya, S. Shrivastava, T. Shripathi, V. Ganesan, Optik, **125**, 6751 (2014).
- [8] Y. Wang, F. Zhang, L. Wei, G. Li, W. Zhang, Physica B, **457**,194 (2015).
- [9] F. Faezeh, H. Sara, Mater. Sci. Appl., **3**, 697 (2012).
- [10] C.-Y. Hsu, W.-T. Chen, Y.-C. Chen, H.-Y. Wei, Y.-S. Yen, K.-C. Huang, K.-C. Ho, C.-W. Chu, J.T. Lin, Electrochim. Acta , **66**, 210 (2012).
- [11] G. Ma, X. Tang, Z. Zhong, H. Zhang, H. Su, Microelectron. Eng., **108**, 8 (2013).
- [12] D. Nguyen, A. Ferrec, J. Keraudy, J. Bernède, N. Stephant, L. Cattin, P.-Y. Jouan, Appl. Surf. Sci., **311**, 110 (2014).
- [13] X.L. Zhang, H.T. Dai, J.L. Zhao, C. Li, S.G. Wang, X.W. Sun, Thin Solid Films, **567**, 72 (2014).
- [14] S. Pereira, A. Gonçalves, N. Correia, J. Pinto, L. Pereira, R. Martins, E. Fortunato, Sol. Energy Mater. Sol. Cells, **120**, 109 (2014).
- [15] P. C. Chou, H. I. Chen, I. P. Liu, C. C. Chen, J.K. Liou, K. S. Hsu, W. C. Liu, Int. J. Hydrogen Energy, **40**, 729 (2015).
- [16] I. Sta, M. Jlassi, M. Kandyla, M. Hajji, P. Koralli, R. Allagui, M. Kompitsas, H. Ezzaouia, J. Alloys Compd., **626**, 87 (2015).
- [17] G. Bodurov, P. Stefchev, T. Ivanova, K. Gesheva, Mater. Lett., **117**, 270 (2014).
- [18] J.P. Kollender, B. Gallistl, A.I. Mardare, A.W. Hassel, Electrochim. Acta, **140**, 275 (2014).
- [19] K.X. Steirer, J.P. Chesin, N.E. Widjonarko, J.J. Berry, A. Miedaner, D.S. Ginley, D.C. Olson, Org. Electron., **11**, 1414 (2010).
- [20] H. Ohldag, N. Weber, C. Bethke, F. Hillebrecht, J. Electron. Spectrosc. Relat. Phenom., **114–116**, 765 (2001).
- [21] Y. Zhang, Appl. Surf. Sci., **344**, 33 (2015).
- [22] M. Krunk, J. Soon, T. Unt, A. Mere, V. Mikli, Vacuum, **107**, 242 (2014).
- [23] H. Wang, G. Wu, X. Cai, Y. Zhao, Z. Shi, J. Wang, X. Xia, X. Dong, B. Zhang, Y. Ma, Vacuum, **86**, 2044 (2012).
- [24] M. Jlassi, I. Sta, M. Hajji, H. Ezzaouia, Mater. Sci. Semicond. Process., **21**, 7 (2014).
- [25] Y. Akaltun, T. Çayır, J. Alloys Compd., **625**, 144 (2015).
- [26] I. Fasaki, A. Koutoulaki, M. Kompitsas, C. Charitidis, Appl. Surf. Sci., **257**, 429 (2010).
- [27] D. Jiang, J. Qin, X. Wang, S. Gao, Q. Liang, J. Zhao, Vacuum, **86**, 1083 (2012).
- [28] S. Chen, C. Wen, T. Kuo, W. Peng, H. Lin, Thin Solid Films, **572**, 51 (2014).
- [29] I. Hotovy, L. Spiess, M. Predanocy, V. Rehacek, J. Racko, Vacuum, **107**, 129 (2014).

- [30] S. Moghe, A. Acharya, R. Panda, S. Shrivastava, M. Gangrade, T. Shripathi, V. Ganesan, *Renew. Energy*, **46**, 43 (2012).
- [31] S. Chen, T. Kuo, Y. Lin, S. Hsu, H. Lin, *Thin Solid Films*, **549**, 50 (2013).
- [32] S. Kerli, U. Alver, H. Yaykaşlı, *Appl. Surf. Sci.*, **318**, 164 (2014).
- [33] A. Dakhel, *J. Non-Cryst. Solids*, **358**, 285 (2012).
- [34] I. Sta, M. Jlassi, M. Hajji, H. Ezzaouia, *Thin Solid Films*, **555**, 131 (2014).
- [35] M.B. Amor, A. Boukhachem, K. Boubaker, M. Amlouk, *Mater. Sci. Semicond. Process.*, **27**, 994 (2014).
- [36] V. Gowthami, M. Meenakshi, P. Perumal, R. Sivakuma, C. Sanjeeviraja, *Mater. Sci. Semicond. Process.*, **27**, 1042 (2014).
- [37] V. Gowthami, P. Perumal, R. Sivakumar, C. Sanjeeviraja, *Physica B*, **452**, 1 (2014).
- [38] A. Boukhachem, R. Boughalmi, M. Karyaoui, A. Mhamdi, R. Chtourou, K. Boubaker, M. Amlouk, *Mater. Sci. Eng., B* **188**, 72 (2014).
- [39] A.A. Al-Ghamdi, M.Sh. Abdel-wahab, A.A. Farghali, P.M.Z. Hasan, *Mater. Res. Bull.*, **75**, 71 (2016).
- [40] M.V. Kumar, S. Muthulakshmi, A.A. Paulfrit, J. Pandiarajan, N. Jeyakumaran, N. Prithivikumaran, *Int. J. Chem. Tech. Res.*, **6**, 5174 (2014).